Shallow, high-resolution converted-wave seismology for coal exploration

Steve Hearn *
Velseis Pty Ltd and
University of Queensland, Australia
steveh@velseis.com.au

SUMMARY

Despite the considerable successes of multi-component seismology in the petroleum industry, there has been relatively little effort devoted to shallow, high-resolution converted-wave imaging in the coal sector. By analogy to petroleum-scale applications, converted-wave imaging in the coal environment offers interesting possibilities for independent validation of mapped structures, clearer imaging in the shallow sub-surface, and detection of gas, sandstone channels and/or fracture swarms.

Over the past two years Velseis Pty Ltd has conducted the first experiments in Australia to utilise shallow, high-resolution multi-component data and converted-wave technology to image coal seams. Three 2D multi-component coal-seismic datasets have been acquired in the Bowen Basin, Australia. Only minimal changes to conventional recording equipment and procedures have been required. A conventional dynamite source has been used, with a single, multi-component geophone replacing the conventional array of vertical geophones at each receiver.

Converted-wave processing algorithms developed within the petroleum sector have been successfully applied to the three trial datasets. This has involved specialised approaches to S-wave receiver statics, PS normal moveout and common conversion-point binning. Considerable experimentation to fine tune processing parameters and the converted-wave processing sequence has been necessary for optimum handling of the shallow, high-resolution data. Overall the processing of the PS data has been significantly more challenging, and has required more geological input, than conventional P-wave processing.

This research has demonstrated that converted-wave imagery is viable in the shallow environment. The derived PS images can extend the interpretation achieved with conventional P-wave images.

Key words: converted-wave seismic, PS imaging, multi-component seismic, 3-C

INTRODUCTION

Multi-component seismology and associated converted-wave (PS) imaging methods have received considerable attention in the petroleum sector. Remarkable advances have been made in multi-component acquisition and processing in recent years, and there are a number of examples where converted-wave seismic techniques have proven more successful than conventional seismic imaging methods (*eg*, Barkved *et al*, 1999; Engelmark, 2001).

In contrast, there has been little effort devoted to shallow, high-resolution converted-wave imaging in the coal sector. This is despite the knowledge that coal seams generate particularly strong converted waves (*eg*, Fertig and Müller, 1978; Greenhalgh *et al*, 1986). Converted-wave imaging in the coal environment has the potential to provide independent validation of mapped structures and clearer or more coherent sub-surface images. By analogy with petroleum-scale applications, there are also interesting possibilities for detection of gas, sandstone channels and/or fracture swarms.

Over the past two years Velseis Pty Ltd has conducted the first experiments in Australia to utilise shallow, high-resolution multi-component seismic data and converted-wave technology to image coal seams (Velseis, 2003). To date, three 2D multi-component coal-seismic datasets have been acquired in the Bowen Basin, Australia. This paper summarises the initial stages of our research. It demonstrates that converted-wave imagery is viable in the shallow coal environment, and that it can extend the results achieved with conventional P-wave reflection.

MULTI-COMPONENT ACQUISITION

Converted-wave seismology is an efficient acquisition strategy which can accommodate both P-wave and PS-wave recording through use of a conventional P-wave seismic source. The data considered here have been acquired using a buried dynamite source, and only minimal changes to conventional recording equipment and procedures have been required to take advantage of PS energy arriving at the surface. The primary difference is the receiver device.

S waves are very sensitive to lateral variations in the near surface. Hence, geophone arrays of any length can severely distort the S-wave energy arriving at the surface (*eg*, Hoffe *et al*, 2002). Consequently, the data presented here have been acquired using only a single, multi-component geophone at each receiver station. This replaces the array of vertical geophones used for conventional acquisition. Note that our field experiments indicate that single-geophone acquisition does not compromise the quality of the conventional P-wave data.

Figure 1 shows a representative record (vertical and inline components) from Field Trial #1. These data have been acquired in an area that has a single, thick coal seam at relatively shallow depths. On the vertical component the P-wave reflection from

the target coal seam is at 0.1 s at zero offset. The strong PS reflection event on the inline component (0.2 s – 0.25 s on centre traces) demonstrates strong conversion is occurring at the target coal seam. Unfortunately, the event coherency seen on this inline shot record is not typical. More typically, the raw inline shot records show poor reflection coherency due to severe receiver-related statics. Such time shifts are caused by significant lateral variations in the S-wave velocity of the near-surface material. As discussed below, removal of such statics is non-trivial but critical to the success of converted-wave imaging. Note also that the inline record suffers from greater surface-related noise compared to the vertical record. This is typical of all three multi-component datasets. As a consequence, the final PS images suffer from poorer signal-to-noise ratios than conventional P-wave images.

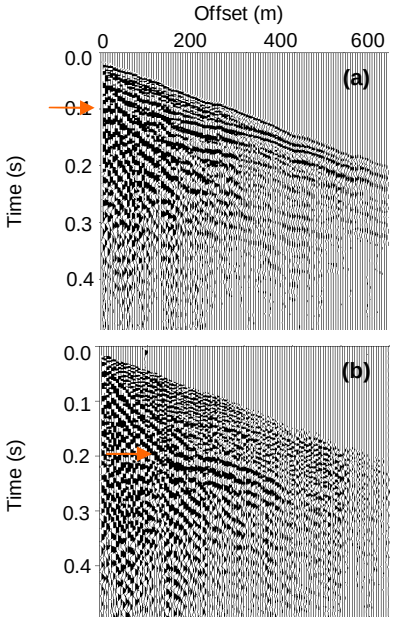

Figure 1. (a) Vertical component and (b) inline component of a representative shot record from Field Trial #1 acquired in the Bowen Basin, Australia. The target P and PS reflection events are indicated.

CONVERTED-WAVE PROCESSING

Processing of converted-wave seismic data involves a number of steps that are substantially different from, and significantly more challenging than, conventional P-wave processing. In particular, converted-wave processing involves specialised approaches to S-wave receiver statics, PS normal moveout (NMO) correction and common conversion-point (CCP) binning.

S-Wave Receiver Statics

S-wave receiver static corrections are required to compensate for delays associated with converted S-wave energy travelling through the weathered surface layer. S-wave receiver statics are generally not related in any way to the conventional P-wave receiver statics. This is due to differences in the effective thickness of the near-surface low-velocity layer for P and S waves (since S waves do not respond to the water table), and the fact that S velocities in the surface layer can be up to ten times smaller than P velocities. As illustrated by Figure 2, S-wave receiver statics in practice are generally much larger than P-wave receiver statics, and vary much more significantly from location to location.

Practical experience has demonstrated that the accurate computation of S-wave receiver statics is particularly important to the success of stacking shallow, high-resolution converted-wave data. To date, we have trialled two different approaches to computing S-wave receiver statics. Both use the common-receiver gather (CRG) stack generated from the inline component of data, following correction of the P-wave shot statics. The first approach for computing S receiver statics simply involves hand picking time shifts between traces in the CRG stack. The second approach uses the automatic CRG stack-power optimisation method of Cary and Eaton (1993). To preserve known structure and dip, the two-way time structure from the conventional P-wave image, scaled by a suitable *Vp*/*Vs* ratio (where *Vp* is P-wave velocity and *Vs* is S-wave velocity), is used to remove structure and dip from the CRG stack prior to any static computations.

Note that both methods of static computation recover only relative S-wave receiver statics. For shallow imaging it is critical to manually shift the PS data back to a surface datum so that the P-wave velocities used subsequently in the processing flow are properly aligned in time. This can be approximately achieved by forcing the smallest S-wave receiver static to be zero and shifting all other statics relative to this. Despite the logistical advantage of the automated statics method, we have found that it is susceptible to cycle-skipping in noisy data. Hence the labour-intensive, hand-picking method is our current preferred approach. In practice, several iterations of S-wave receiver statics computations must be undertaken to optimise the static corrections.

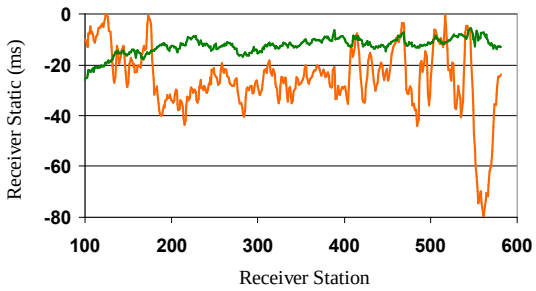

Figure 2. Comparison of conventional P-wave receiver static corrections (green) and S-wave receiver static corrections (orange) for Field Trial #3. The S-wave receiver statics are much larger and more variable than the corresponding P-wave receiver statics.

PS NMO and CCP Binning

PS reflection events exhibit non-hyperbolic NMO which is dependent on *Vp*, *Vs*, the depth of the reflector and the horizontal distance from the source point at which the conversion occurs (*eg*, Zhang, 1996). P-wave velocities (*Vp*) are extracted from conventional P-wave processing of the vertical component of data. Velocity analysis for converted-wave data is designed to recover S-wave velocities (*Vs*) or equivalently the P-wave to S-wave velocity ratio (*Vp*/*Vs*). Our preferred velocity analysis tool produces a suite of constant

Vp/*Vs* stacks and involves re-binning the data for each trial velocity ratio. (This approach is analogous to using conventional constant-velocity stacks.) We have found it necessary to handle positive and negative offsets independently so as to work around the diodic (ie, non-symmetric) moveout observed in CCP gathers. Such behaviour may be related to anisotropy (*eg*, Thomsen, 2002). Consequently, our final PS sections consist of zones of traces created from stacking either positive or negative offset traces. We have also found that it is critical for *Vp*/*Vs* to vary smoothly along the line to avoid spurious binning artifacts.

The raypath of a PS wave through the Earth is asymmetric. This is because the upcoming S wave travels more steeply than the downgoing P wave. Consequently, the reflection point of a PS wave is offset from the midpoint of the source and receiver, towards the receiver. The precise location of this reflection point is actually a function of *Vp*/*Vs*, and will vary with the depth of the reflector. The process of forming common-conversion point gathers is referred to as CCP binning.

Two different approaches to CCP binning have been trialled during this research. The first, here referred to as horizon-based CCP binning, assumes that there is only one target horizon for which the traces must be optimally binned. This method has been used for Field Trials #1 and #3, since there is only one target coal seam. The binning algorithm scans for the supplied two-way time of the PS target reflection event, and the *Vp*/*Vs* at that two-way time on each trace, and computes the CCP for those specific parameters. Shallower and deeper reflectors in the PS image will inevitably be smeared and mispositioned by this approach. The second method of CCP binning is more suitable when multiple reflection events must be accurately imaged, and is here referred to as dynamic CCP binning. This latter approach bins each sample down each trace according to its two-way time and the local *Vp*/*Vs* value. Thus portions of seismic traces can be assigned to different CCP bin locations, and contribute to different traces in the final stacked section. This binning approach has been used for Field Trial #2, which incorporates multiple target horizons.

INTERPRETIVE RESULTS

As suggested by the above discussion, processing of our converted-wave data has proven non-trivial. Nevertheless, viable PS images have been achieved for all three trial multi-component surveys. Here we comment on some of the more interesting interpretive results.

Field Trials #1 and #3 have been conducted over similar single coal-seam geologies, and the overall PS image quality for the two experiments is comparable. Figure 3 shows the P and PS images for Field Trial #3. As is conventional practice, the vertical scale of the PS image has been adjusted (based on an estimated *Vp*/*Vs* ratio) to provide a comparable depth perspective to the P-wave image. The PS image is competitive for structural imaging, providing independent validation of the major structural features. Two of the structural features interpreted on the PS image in Figure 3 (marked in orange) would prompt re-evaluation of the original P-wave interpretation.

One attraction of converted-wave reflection is that S wavelengths can potentially be shorter than for P-waves, since S-wave velocities are slower. This could lead to resolution advantages. However, for a PS image to yield a higher-resolution image of the sub-surface, the dominant frequencies on the PS image have to be competitive with those seen on the P-wave image. For our three trials to date, we have seen a reduced dominant frequency on the PS image, leading to no significant resolution advantage. This reduced frequency content is visible on the field records, indicating greater attenuation and/or scattering of the upcoming S-wave energy. The frequency content on the final stacked section is further compromised by more severe static problems, as discussed above. As a result, we observe that for Field Trials #1 and #3, the net resolution on the PS images is comparable to that seen on the P-wave images.

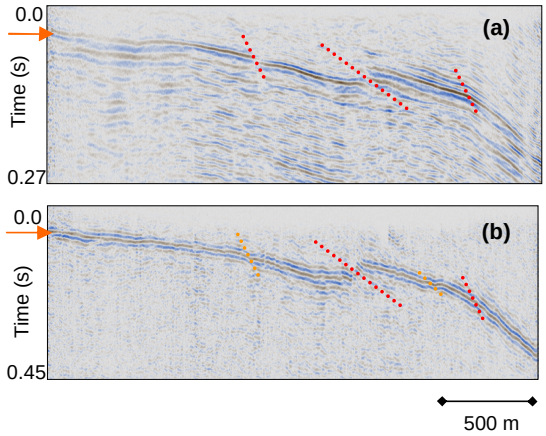

Figure 3. (a) Conventional P-wave image and (b) converted-wave (PS) image derived from Field Trial #3. The target coal seam reflection events are indicated by the orange arrows. Interpreted faults are approximately marked. Faults marked in orange on the PS image may or may not correlate directly with structures observed on the P-wave image.

Perhaps the most interesting result achieved for Field Trial #3 is observed along the left-most end of the line, where the target coal seam is very shallow. In this region, the P-wave image (Figure 3(a)) is sub-optimal, such that structure in the coal seam cannot be reliably interpreted. This poor P-wave image is primarily a geometric effect caused by refracted arrivals interfering with the shallow reflection event. One of the recognised potential benefits of converted-wave imagery is in such shallow situations (*eg*, Garotta, 1999). Since the PS reflection event has a larger travel time, it is less prone to interference from refracted arrivals, such that a higher fold stack is achievable. This proposition is exemplified in the PS stack of Figure 3(b), where the shallow seam can be easily tracked to the extreme left of the section. The PS image predicts that the target seam is essentially free of significant structure in this region.

Field Trial #2 was carried out in a multi-seam environment. In this case, the dominant frequency on the PS image was significantly reduced in comparison to the P-wave image, yielding a net reduction in resolution (Figure 4). In this instance, the PS image does not add significantly to the structural interpretation. However, this multi-seam example does illustrate the potential of using integrated P/PS imagery for lithological interpretation. In Figure 4 significant geological interfaces have been identified on both the P and PS images. Corresponding time intervals have been measured to yield interval *Vp*/*Vs* ratios. Figure 5 shows the lateral variation in *Vp*/*Vs* for the three

geological intervals of interest. The uppermost interval (green) exhibits generally high *Vp*/*Vs* ratios, as might be expected in the shallower, less-consolidated part of the section. The second interval (blue) exhibits an abrupt lateral change in *Vp*/*Vs* (around CDP 700). This is consistent with a change from shale-rich material on the right to sandy (or possibly gas contaminated) material on the left. The deepest interval (red) lies immediately above the target coal seam. This exhibits a more consistent *Vp*/*Vs* ratio, indicative of a shale-rich sequence. Lithological conclusions such as these are relevant in mine planning.

CONCLUSION

This case study represents the first significant evaluation of converted-wave technology in the Australian coal environment. Combined P/PS datasets have been recorded with minimal adjustment to standard P-wave acquisition procedures. Processing of our converted-wave data has proven challenging, particularly in the definition of severe S-wave receiver statics. Nevertheless viable PS images have been obtained. In two of the three trials, the PS image has proven competitive for structural imaging, providing independent validation of features. The PS image has demonstrated significant advantage in imaging a very shallow coal seam. A converted-wave trial in a multi-seam environment has illustrated the potential of integrated P/PS imagery for lithological interpretation. Currently, the cost of an integrated P/PS dynamite survey is some 30% greater than for a standard P-wave survey. This case study suggests that, as the technology is refined, this impost could be justified in terms of increased information content.

ACKNOWLEDGMENTS

This research received financial support from the Australian Coal Association Research Program (ACARP Project C10020).

REFERENCES

Barkved, O.I., Mueller, M.C., and Thomsen, L., 1999, Vector interpretation of the Valhall 3D/4C OBS dataset: 61st Conference and Technical Exhibition, EAGE, Extended Abstracts, #6-42.

Cary, P.W., and Eaton, D.W.S., 1993, A simple method for resolving large converted-wave (P-SV) statics: Geophysics 58, 429-433.

Engelmark, F., 2001, Using 4-C to characterise lithologies and fluids in clastic reservoirs: The Leading Edge 20, 1053-1055.

Fertig, J., and Müller, G., 1978, Computation of synthetic seismograms for coal seams with the reflectivity method: Geophysical Prospecting 26, 868-883.

Garotta, R., 1999, Shear Waves from Acquisition to Interpretation: 2000 DISC, SEG, Oklahoma.

Greenhalgh, S.A., Suprajitno, M., and King, D.W., 1986, Shallow seismic reflection investigations of coal in the Sydney Basin: Geophysics 51, 1426-1437.

Hoffe, B.H., Margrave, G.F., Stewart, R.R., Foltinek, D.S., Bland, H.C., and Manning, P.M., 2002, Analysing the effectiveness of receiver arrays for multicomponent seismic exploration: Geophysics 67, 1853-1868.

Thomsen, L., 2002,. Understanding Seismic Anisotropy in Exploration and Exploitation: 2002 DISC, SEG, Oklahoma.

Velseis, 2003, Investigation of converted-wave seismic reflection for improved resolution of coal structures – Final Report: ACARP Project C10020.

Zhang, Y., 1996, Nonhyperbolic converted-wave velocity analysis and normal moveout: 66th Annual International Meeting., SEG, Expanded Abstracts, 1555-1558.

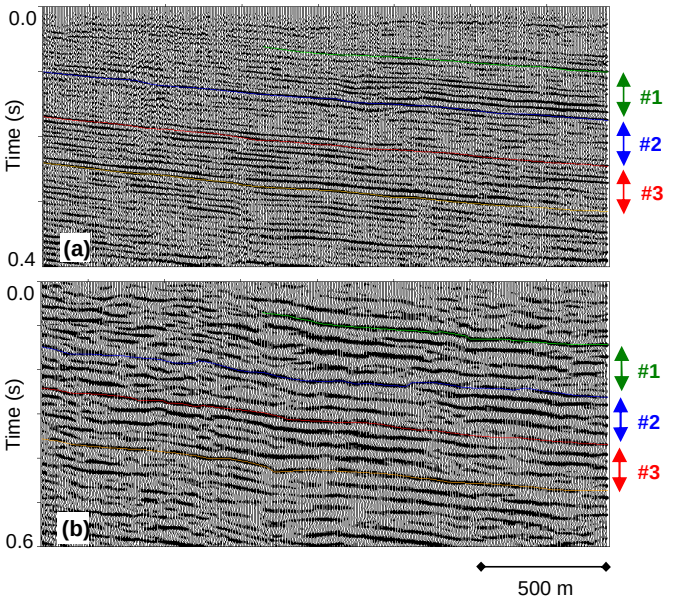

Figure 4. (a) Conventional P-wave image and (b) converted-wave (PS) image derived from Field Trial #2. Interpreted horizons are indicated. Three geological intervals have been defined.

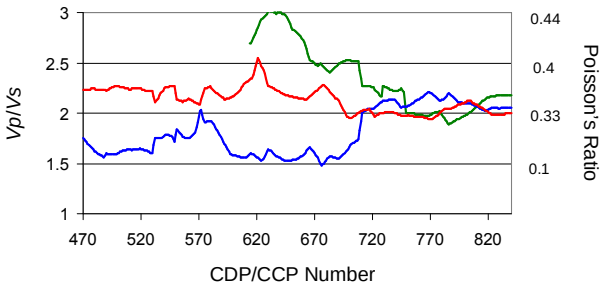

Figure 5. *Vp*/*Vs* for Interval 1 (green); Interval 2 (blue); and Interval 3 (red) interpreted on the P and PS images show in Figure 4. A high *Vp*/*Vs* (greater than 2.2) corresponds to shale-rich layers or poorly consolidated material. A low *Vp*/*Vs* (less than 1.6) is indicative of high sand and/or gas content. As indicated on the right-hand axis, *Vp*/*Vs* is related to Poisson's Ratio.